

## Sudden Emergence of Redox Active *Escherichia Coli* Phenotype: Cyclic Voltammetric Evidence of the Overlapping Pathways

Xuan-Hui Xie, Erin Lin Li and Zi Kang Tang\*

Nano Science and Technology Program, Hong Kong University of Science and Technology, Clear Water Bay, Kowloon, Hong Kong  
E-mail: [bionanoust@gmail.com](mailto:bionanoust@gmail.com)

Received: 7 July 2010 / Accepted: 15 July 2010 / Published: 10 August 2010

---

Under anaerobic and static culture condition, *Escherichia coli* K-12 (*E. coli*) biofilm was adapting electrochemically on gold electrode in well-defined redox environments modulated by a computerized potentiostat. The electrochemical property of the biofilm/electrode interface was investigated during the 168 h of biofilm adaptation. In-situ cyclic voltammogram (CV) revealed a sudden transition into redox active phenotype after 24 h incubation at 0 V and 0.2 V, which seems to be controlled by quorum-sensing mechanism. Further analysis of CV results implies the kinetic details of extracellular respiration. The simultaneous linear dependence of the peak current on the scan rate and the square root of the scan rate suggest the coexistence of surface and diffusion controlled process which was likely due to the overlapping pathways of direct and indirect electron transport. It is for the first time that the mixed controlled regime has been observed at cellular level. To gain further insight in to the redox active adaptation, cellular redox state was monitored through out the course. Although in the natural condition where the redox environment was not artificially controlled *E. coli* adapted towards lower cellular redox state that thermodynamically favored the electron transport, it did not evolve to redox active phenotype. Similar trends of adaptation of cellular redox state towards lower potential were observed in the 0 V and 0.2 V redox environments. Moreover, differentiated early stage response in cellular redox state suggests parallel adaptation processes which were eventually dominated by extracellular respiratory activity as indicated by the convergence of the mixed cellular potential to the redox midpoint potential in the later stages of adaptation.

---

**Keywords:** Directed redox adaptation, *E. coli*, extracellular electron transport, overlapping pathways, mixed cellular potential

### 1. INTRODUCTION

Redox reactions are pivotal to cellular metabolism [1-5]. Under varying environmental redox conditions, the ability to tune up cellular redox state such that a variety of cellular processes could

optimize their function constitutes an essential part of homeostasis [6, 7]. Cellular redox state is conventionally determined by redox electrode through which the electrostatic potential is recorded [8-10]. However, this apparent mixed potential results from equilibrium of the ensemble of redox active and inactive species [11-13]. It is hard to distinguish the potential of the redox functional components of interest from the others.

Unlike eukaryotes that could spatially isolate redox-interfering reactions in membrane-bounded cell compartments, unicellular bacteria have to devise alternative strategies to respond to the alterations of environmental redox potential to optimize their physiological fitness [14]. However, what metabolic adaptation subsequently occurs in well-defined redox environment has not been well understood. On one hand, the multitude of regulatory pathways at the level of transcription [15] obscures the underlying redox responsive modules [16]; on the other hand previous works use excessive chemical substances of specific redox potential to alter and control the environmental redox state [1]. This methodology often confounds the results in that the chemical substances not only affect the cellular redox state but also potentially act as signaling molecules that chemically interact with cellular machinery including the electron transport chain [1].

Despite a plethora of studies on the electron transport from enzymes to electrode [17], mechanistic study on the electron transport at the whole cell level is relatively scarce, which is primarily due to the complexity of cellular redox activities that interfere each other and confound the understanding of specific process. We have previously modulated and monitored *E. coli* biofilm formation by EQCM and EIS methods [18, 19]. In this study, we focused on the kinetic details of the emergent extracellular electron transport activity using CV. We investigated the history of phenotypic adaptation of *E. coli* under anaerobic and static culture condition. In specific, both the extracellular electrochemical activity and redox state were monitored throughout the course in different conditions. A computerized potentiostat was employed to modulate the environmental redox state on the working electrode against the reference electrode, by which the evolved redox active phenotype could also be examined in-situ. Adaptations were directed at physiologically relevant environmental redox potential of 0 V and 0.2 V that mimic electron acceptors dimethyl sulfoxide (DMSO) and nitrate, respectively. As a control, adaptation in the natural anaerobic condition where the environmental redox potential was not maintained was run in parallel. CV and the mixed cellular potential have been recorded throughout the course of redox adaptation. Analysis of the redox peak was carried out to elucidate the kinetics of the electron transport. It is crucial to distinguish the redox midpoint potential of the extracellular electron transport components from the mixed cellular potential determined by the ensemble of extracellular components in order to gain insight into the adaptation process of interest.

## 2. EXPERIMENTAL PART

### 2.1. Bacterial preparation

Wild type *E. coli* culture was grown under aerobic condition in Luria-Bertani (LB) medium (Peptone, 10 g/L; yeast extract, 5 g/L; NaCl, 10 g/L) at 30 °C at 150 rpm. The growth of *E. coli* was

monitored by Optical Density at 600 nm ( $OD_{600}$ ) using Ultrospec 4300 pro UV/Visible Spectrophotometer (GE) with cuvettes of 1-cm path length. Culture was harvested at mid log-phase and diluted with fresh LB medium. Bacterial concentrations were adjusted for each experiment to give a final concentration of  $OD_{600} = 0.3$  for immediate use. All chemicals are analytical grade and used as received from Sigma Aldrich.

## 2.2. Electrochemical characterizations

Three-electrode configuration was adopted for electrochemical characterizations. Gold disc electrode was used as working electrode. Pt wire and Ag/AgCl (saturated KCl) were used as counter and reference electrode, respectively. Prior to use, working and counter electrodes were cleansed with piranha solution (70%  $H_2SO_4$  and 30%  $H_2O_2$ ) and thoroughly rinsed with Milli-Q water. Reference electrode was sterilized by 75% ethanol solution. Airtight and autoclaved chambers of identical configuration were used for adaptation experiments. All adaptation experiments were performed at 22 °C. Unless otherwise stated, potentials were referred to Ag/AgCl (saturated KCl).

Before introducing into the electrochemical chamber, *E. coli* culture and the chamber were thoroughly purged with nitrogen streams to create anaerobic condition. To direct adaptation of *E. coli*, a computer controlled PAR 283 potentiostat (EG&G Princeton Applied Research) was used to maintain the potential on the working electrode against reference electrode at 0 V and 0.2 V. To mimic natural anaerobic adaptation, control experiments were performed using the same setup except that the potential on the working electrode was not artificially controlled. During the course of adaptation, the mixed cellular potential of *E. coli* was determined by measuring the open circuit potential of the working electrode. CVs were obtained to evaluate the emergence of electrochemically active phenotype. Peak analysis of the CVs was using UTILS software.

## 2.3. Microscopic observation of biofilm on electrode

After the 168 h biofilm adaptation experiment, the working electrodes were taken out of the electrochemical chambers and rinses three times with Milli-Q water to make sure that the remaining cells were firmly attached to the electrodes. The surface colonizing biofilm cells were then observed under Olympus BX51 microscope. Images were captured with 500 × total magnification.

# 3. RESULTS AND DISCUSSION

## 3.1. Sudden emergence of redox-active phenotype

*E. coli* has the ability to survive under a wide range of environmental redox conditions through adopting different metabolic modes [20]. Under anaerobic condition, either fermentative glycolysis or extracellular electron transport via self-excreted secondary metabolites [21-23] could be adopted to meet the energetic demand. The secondary metabolites shuttle electrons from electron transport chain

to extracellular electron acceptors such as iron and sulfur. Therefore, the redox activity of electron shuttles could be exploited as fingerprint for the metabolic mode of extracellular respiration.

*E. coli* was incubated in static condition in the electrochemical chamber to allow adaptation and biofilm development on the gold working electrode. CVs were recorded during the adaptation process in the 0 V and 0.2 V environmental redox state and under the natural condition where the environmental redox state was not controlled. As shown in Fig. 1A, the oxidation-reduction peak did not appear in CVs throughout the 168 h anaerobic adaptation, suggesting that *E. coli* adopted fermentative glycolysis under natural anaerobic condition. In contrast, under redox-controlled conditions at 0 V (Fig. 1B), oxidation-reduction peak did not emerge until 24 h and the peak current enlarged subsequently, revealing that the electrochemical activity was continuously enhancing during the redox adaptation. Similar trend of adaptation was observed in CVs of adaptation at 0.2 V (Fig. 1C). It is intriguing that *E. coli* remained redox inactive for 24 h and suddenly transitioned into redox active phenotype, which implies quorum sensing type of sudden transition [24]. This behavior was not observed in previous study of using electrode as terminal acceptor by Wang [23] because flow rather than static condition was adopted. The flowing medium would take away the quorum sensing molecules excreted by bacteria in the extracellular solution. Consequently the signaling molecules cannot reach the critical concentration to trigger the sudden transition. Therefore, the culture condition, especially the water dynamics has intricate influence on redox adaptation.

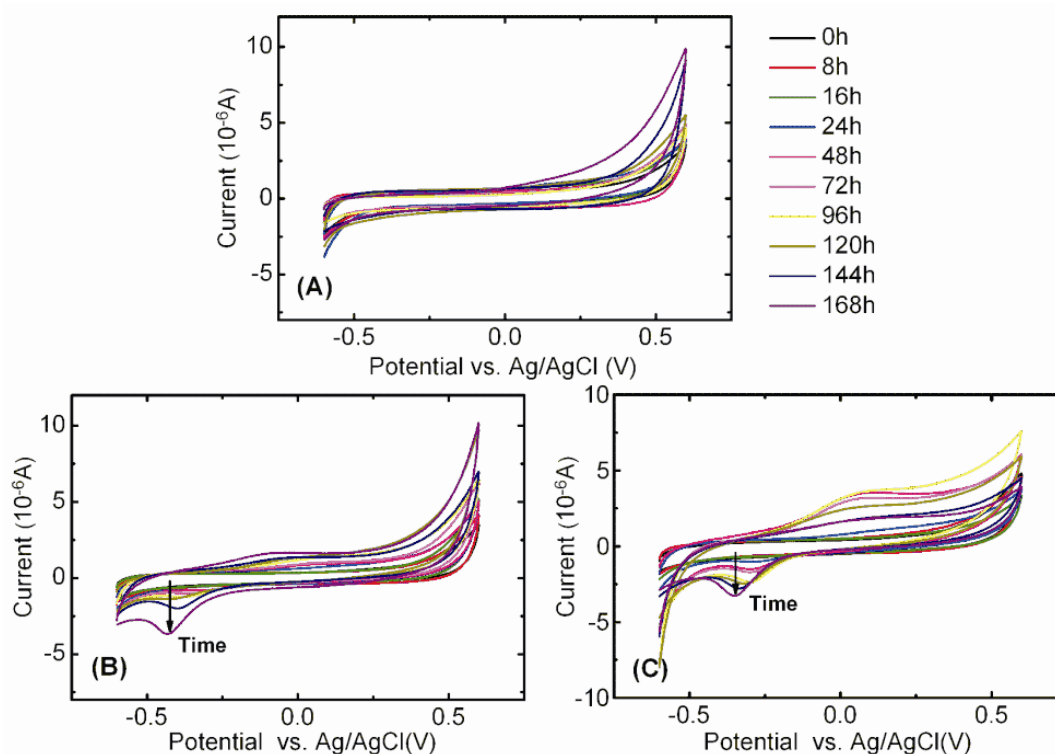


**Figure 1.** Cyclic voltammogram (CV) at a scan rate of  $50 \text{ mV s}^{-1}$  obtained during the 168 h adaptation of *E. coli* under the natural condition (A), in the 0 V (B) and 0.2 V (C) environmental redox state.

### 3.2. Physiological relevance of electrode potential

From the thermodynamic perspective, the formal potential of the upstream electron donors NADH and ubiquinone are  $-320$  mV and  $110$  mV (vs. SHE), respectively, which are equivalent to  $-0.517$  V and  $-0.087$  V vs. Ag/AgCl reference electrode, respectively. Considering that the potential on the electrode was maintained at  $0$  V and  $0.2$  V vs. Ag/AgCl, it is thermodynamically favorable to use the electrode as terminal acceptor. Under anaerobic condition, *E. coli* adopts alternative respiratory pathways to maintain redox balance and cellular energetics. When there is no terminal electron acceptor available intracellularly or extracellularly, it could not exploit the membrane-bounded electron transport chains for energy transduction [25]. Instead, it uses fermentative glycolysis, resulting in disproportionate products [26] such as acetate and ethanol of which electrons are not completely extracted, hence lowering the energetic efficiency. The artificially controlled electrode potential at  $0$  V and  $0.2$  V are close to the formal potential of the redox couples DMSO/DMS ( $-0.037$  V vs. Ag/AgCl) [27] and  $\text{NO}_3^-/\text{NO}_2^-$  ( $0.223$  V vs. Ag/AgCl) [28]. The electrode potential was therefore attempted to mimic the natural terminal electron acceptors DMSO and nitrate, which match the alternative terminal reductases of the electron transport chains, noting that the formal potential of DSMO reductases and periplasmic nitrate reductase are  $-0.037$  V and  $0.223$  V vs. Ag/AgCl, respectively [29]. The adapted redox active phenotype suggests that under anaerobic condition *E. coli* cells are able to use the working electrode as the terminal electron acceptor to establish proton-motive force for energy transduction.

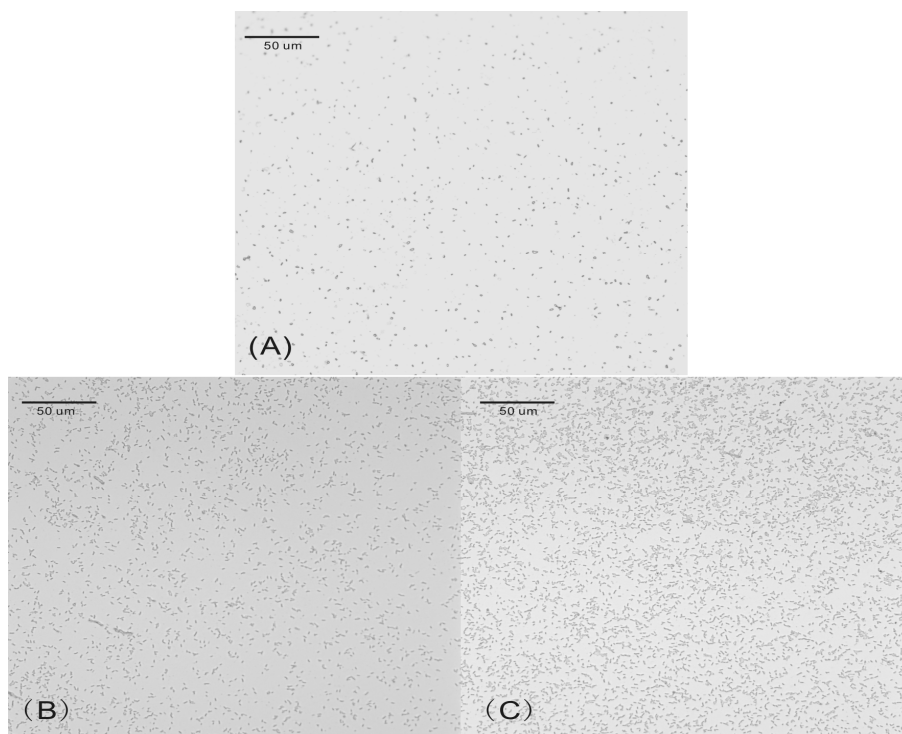


**Figure 2.** Optical microscope images (500 x total magnification) of *E. coli* cells (at 168 h) on the electrodes in the natural (A),  $0$  V (B) and  $0.2$  V (C) conditions.

The microscopic images of *E. coli* on the gold working electrodes are illustrated in Fig. 2. The cell density in the natural condition (Fig. 2A) is much lower than that in the 0 V (Fig. 2B) and 0.2 V (Fig. 2B) conditions. This reflects that metabolism of different energetic efficiency was adopted by cells in the natural and redox-controlled conditions. Furthermore, cell density in the 0.2 V condition is higher than that at 0 V, suggesting that larger voltage drop between electron transport chains and terminal acceptor (electrode) gives rise to larger energetic benefit.

### 3.3. Overlapping pathways

#### 3.3.1. Redox-active secondary metabolites

While the entries of electrons into the electron transport chains are NADH:ubiquinone oxidoreductase (NDH-1) [29] and succinate:ubiquinone oxidoreductase (succinate dehydrogenase) [30], the exit is not unambiguous. The reduction peak current exhibited nonlinear behavior of adaptation (Fig. 3A, B). The peak current represents the activity of extracellular respiratory electron transport, which did not appear until 24 h and then demonstrated sustained increase. This kind of transition implies a quorum-sensing [24] like regulatory scheme, where the sudden transition into redox active phenotype occurs once the signaling molecules reach the critical concentration. The increased extracellular respiratory activity could be attributed to the positive feedback of regulatory network that upregulated the gene expression of terminal reductases and also possibly the biosynthesis of secondary metabolites [31]. The self-excreted electrochemically active secondary metabolites were reported to mediate extracellular electron transport.

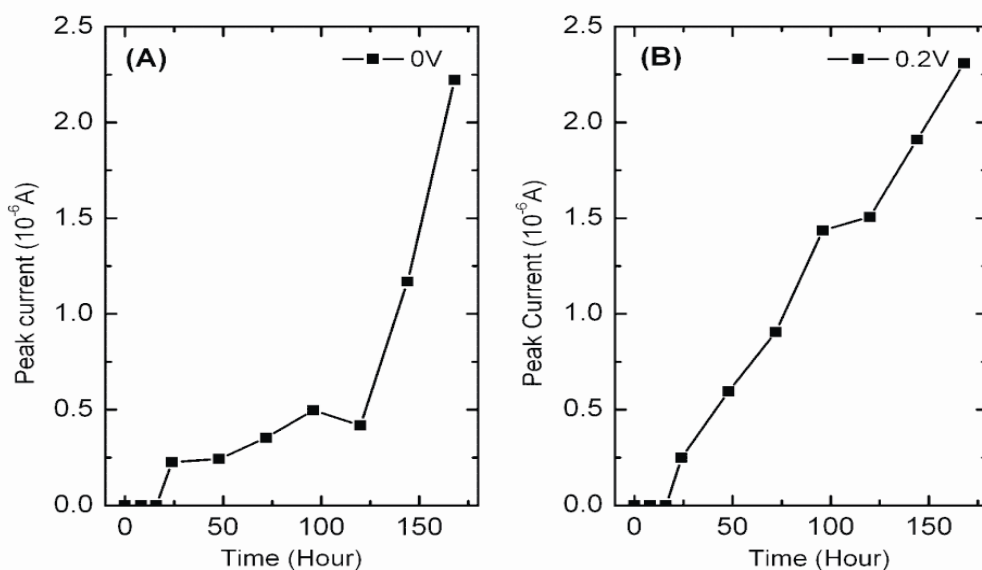


**Figure 3.** Time evolution of reduction peak current of *E. coli* adapted in the 0 V (A) and 0.2 V (B) environmental redox state.

*Pseudomonas aeruginosa*, *Shewanella putrefaciens* and *E. coli* produce diffusible molecules like phenazine [32], flavins [33] and quinone [34] to shuttle respiratorily evolved electrons to external electron acceptors. Alternatively, other species like *Shewanella algae* BrY synthesizes cell-associated melanin [35, 36] to relay electrons to extracellular solid acceptors. Based on the redox peak position (Fig. 1B, C), it is plausible that the mediators are quinone derivatives [22, 23].

The CV results also reveal the kinetic nuance of the extracellular electron transport of *E. coli* cells. A common feature was found in the CVs at 0 V and 0.2 V. The oxidation peak was markedly broadened relative to the reduction peak. The broadening effect reflects active electron transport by cellular machinery of the electron transport chain. During anodic scanning, the potential was ramped from -0.6 V to 0.6 V and mediators were oxidized on the electrode. Therefore, at the proximity of the electrode, the concentration of mediators in reduced state ( $M_{\text{red}}$ ) decreased and mediators in oxidized state ( $M_{\text{ox}}$ ) increased. The oxidation peak appeared as the concentration of  $M_{\text{red}}$  can no longer sustain the anodic current and  $M_{\text{red}}$  in the afar bulk liquid phase cannot timely diffuse to the proximity of electrode to replenish the loss of  $M_{\text{red}}$ . As the upstream cellular machinery of electron transport chain relayed electrons to the mediators,  $M_{\text{ox}}$  was partially back converted into  $M_{\text{red}}$  during scanning, which consequently compensates the depletion of  $M_{\text{red}}$  and delays the diminishing of oxidation peak and hence broadens the peak. Similarly, during cathodic scanning, depletion of  $M_{\text{ox}}$  could be accelerated by cell-donated electrons. The sharpening of reductions peak could be attributed to the coupling of cell-originated and electrode-originated cathodic current during reverse ramping from 0.6 V to -0.6 V. It can be inferred that the electron transfer rate from the upstream donors to the mediators was fairly large and comparable to the scanning rate ( $50 \text{ mVs}^{-1}$ ).

### 3.3.2. Surface and diffusion controlled process

While the highly asymmetric feature of reduction and oxidation peak width of CVs suggests fast kinetics of electron transport, seemingly contradictory result is implied by the rather large peak separation. This feature has also been observed in previous study and the large peak separation is not necessarily indicator of irreversibility of electron transport (slow kinetics) [37]. To further scrutinize the electron transport kinetics. CVs were obtained at a wide range of scanning rate for 0 V (Fig. 4A) and 0.2 V (Fig. 4B) adapted *E. coli* cells. For both conditions, reduction peak current shows linear dependence on the scan rate with linear correlation coefficient 0.946 for 0 V (Fig. 5A) and 0.972 for 0.2 V (Fig. 5C), a characteristic feature of surface controlled process [38-40]. Intriguingly, the reduction peak current also exhibits linear dependence on the square root of the scan rate with linear correlation coefficient 0.924 for 0 V (Fig. 5B) and 0.999 for 0.2 V (Fig. 5D), a characteristic feature of diffusion controlled process [41-45]. The coexistence of surface and diffusion controlled process have also been observed in electron transport from metalloenzyme [37] and dopamine molecules [46, 47] to electrode, but not discovered at cellular level. Microorganisms evolved different strategies to coordinate electron transport to excellular solid phase acceptors. These strategies may overlap by sharing the common node of electron transport chain such as *cymA* (a cytoplasmic membrane-associated periplasmic c-type cytochrome) and menaquinone [48]. When the cellular machinery such

as the membrane-bounded multiheme outer membrane complex [49] and melanin [35, 36] are accessible to the electrode, direct electron transfer is enabled and the redox current of CV is in the surface controlled regime.

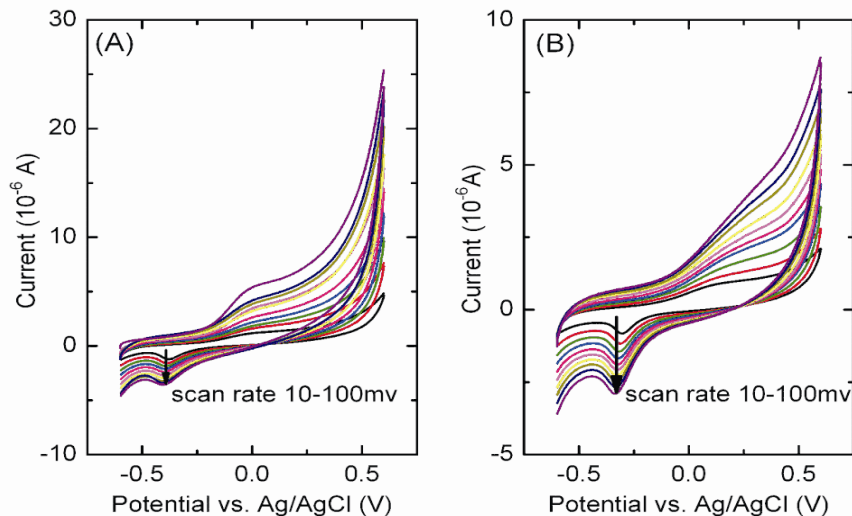


**Figure 4.** Cyclic voltammogram (CV) of *E. coli* adapted in the 0 V (A) and 0.2 V (B) environmental redox state at a series of scan rate from  $10 \text{ mV s}^{-1}$  to  $100 \text{ mV s}^{-1}$ .

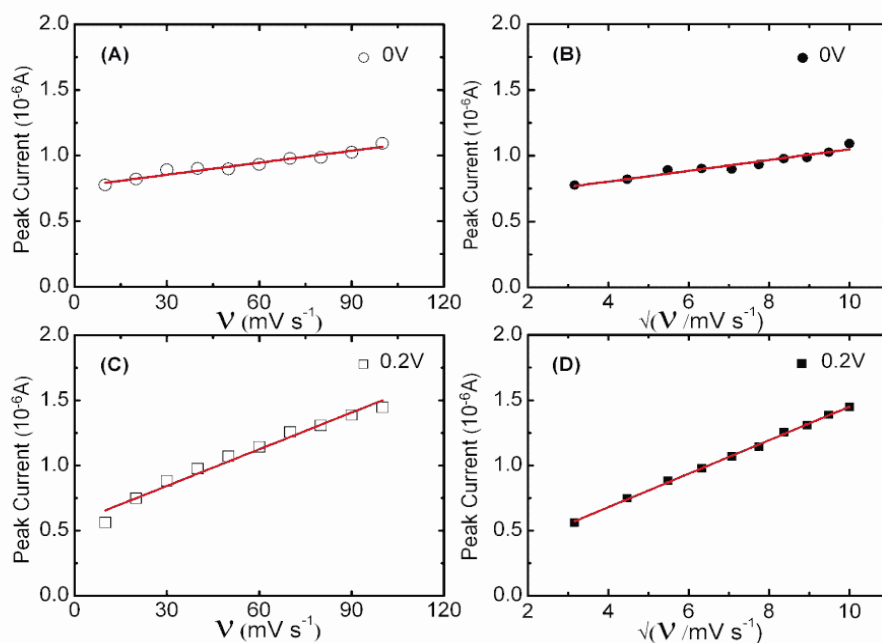


**Figure 5.** Reduction peak current vs. scan rate in the 0 V (A) and 0.2 V (C) environmental redox state. Reduction peak current vs. square root of scan rate in the 0 V (B) and 0.2 V (D) environmental redox state.

Concurrently, low molecule weight molecules such as phenazine, flavins and quinine are able to diffuse between cells and electrode, resulting in diffusion controlled redox current in CV.

The simultaneous linear dependence of reduction peak current on the scan rate and the square root of the scan rate implies mixed controlled regime that both surface and diffusion controlled electron transport were present as a result of the overlapping pathways of direct and indirect extracellular electron transport [50]. The combination of different pathways may endow *E. coli* metabolic plasticity that could utilize a wide range of electron acceptors at a multitude of spatial distributions and of different thermodynamic and kinetic features [29]. Moreover, the broadened oxidation peak width deviated from Gaussian distribution of formal potential [51], which also reflects the inhomogeneous nature of electron transport [52]. The dispersion of rate constant arises from membrane and electrode surface associated processes [52-54]. From the energetic point of view, the inhomogeneity of rate constant reflects the dispersion of reorganization free energy [54, 55] resulted from subdiffusion across membrane pores and nonuniformity of cell adlayer on the electrode [56].

### 3.4. Redox midpoint potential and mixed cellular potential

Processes of different rate constant have their own optimal redox potential for the function of corresponding enzymes, which equilibrate at the mixed cellular potential [11-13]. To gain insight into the optimal redox potential of interested process, it is crucial to distinguish the redox midpoint potential of specific process from the mixed cellular potential. The mixed cellular potential was determined by the electrostatic potential of the working electrode intermittently during the time course of adaptation in the natural and 0 V and 0.2 V redox environment.

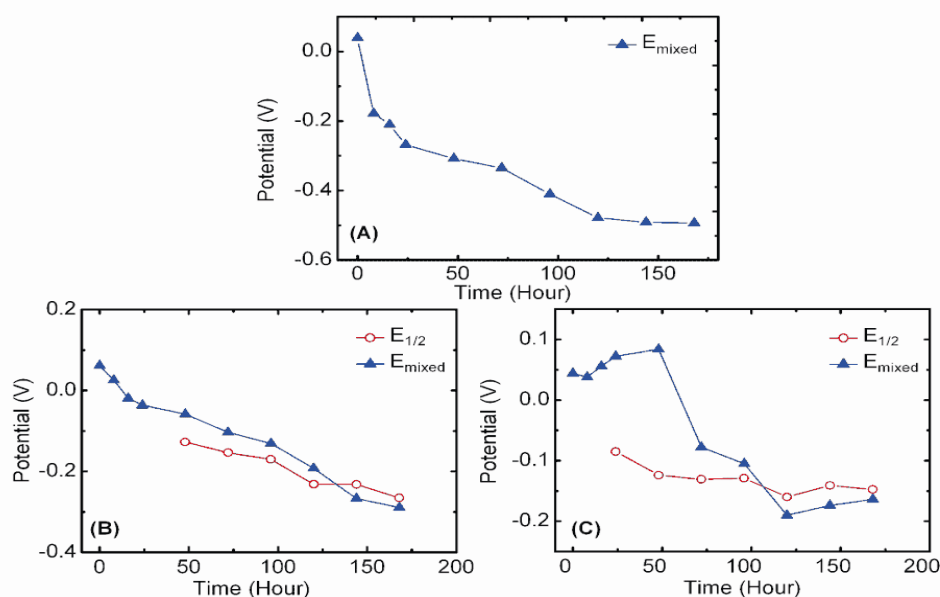


**Figure 6.** Time evolution of the redox midpoint potential ( $E_{1/2}$ ) and mixed cellular potential ( $E_{mixed}$ ) of *E. coli* under the natural condition (A), in the 0 V (B) and 0.2 V (C) environmental redox state.

The redox midpoint potential of the extracellular electron transport was determined from the CV results where oxidation and reduction appeared.

As shown in fig. 6A, under the natural anaerobic condition, the mixed cellular potential exhibited a trend of adaptation towards lower redox state. These results substantiate that although cellular adaptation towards lower redox state is a naturally-occurring phenomenon that favors thermodynamically the electron transport from cells to electrode, it is not sufficient to confer *E. coli* extracellular redox activity.

In the 0 V redox environment, similar adaptive trend of the mixed cellular potential was observed (Fig. 6B). Moreover, the redox midpoint potential shifted negatively in pace with the mixed cellular potential. Interestingly, the gap between the mixed cellular potential and the redox midpoint potential shrunk during adaptation. The mixed cellular potential is determined by all cellular components exposing to the electrode, including not only redox active components that contribute to extracellular respiration such as electron-mediating secondary metabolites, cytochromes and proteins but also redox inactive components such as phospholipids [57] on the cell surface. Therefore, mixed cellular potential is the overall measure of redox active and inactive components. In contrast, redox midpoint potential as determined from CV represents only redox active components that contribute to extracellular respiration. Convergence of the mixed cellular potential to the redox midpoint potential reveals the increased fraction of electroactive components and enhanced electrochemical activity, which was also substantiated by the enlarged peak current (Fig. 3A, B). In the 0.2 V redox environment (Fig. 6C), mixed cellular potential significantly deviated from the redox midpoint potential from 24 h to 48 h, after which the gap gradually shrunk. This feature indicates the occurrence of parallel cellular processes during the early stages of redox adaptation. At later stages, the mixed cellular potential converged to the redox midpoint potential, suggesting that extracellular respiratory activity finally dominated the redox regime.

#### 4. CONCLUSIONS

Under anaerobic and static culture condition in-situ CV results obtained during the time course of adaptation suggest a quorum-sensing like sudden emergence of redox activity in the 0 V and 0.2 V artificially controlled redox environment but not in the natural condition, which has not been observed in previous flow culture condition. Peak analysis of CVs reveals simultaneous linear dependence of peak current on the scan rate and the square root of the scan rate. This intriguing feature denotes the presence of surface and diffusion controlled electron transport process which should be attributed to the overlapping pathways of direct electron transport via membrane-associated terminal reductases like multiheme cytochromes and indirect electron transport mediated by diffusible low molecule weight molecules. It is for the first time that the mixed regime is observed at cellular level.

Based on the peak position, the diffusible mediators are quinone derivatives which are redox active secondary metabolite. The broadening of oxidation peak of CVs suggests active electron transport from the electron transport chain of *E. coli* cells to the electrode. It also reveals the dispersion of electron transfer rate constant, which is possible due to the spreading of reorganization free energy

caused by inhomogeneous surface structure of cells and adlayers on the electrode. Although *E. coli* cells adapted to lower redox state under the natural anaerobic condition, they did not evolve extracellular respiratory pathway. The same trend of mixed cellular redox potential that was determined by the ensemble of cellular redox active and inactive components was observed in *E. coli* cells in the 0 V redox environment, which gradually converged to the redox midpoint potential that represents the redox active cellular component only. Furthermore, differentiated redox adaptation was observed, unlike that at 0 V, the mixed cellular redox potential of *E. coli* at 0.2 V exhibited a bimodal trend, which deviated from the redox midpoint potential from 24 h to 48 h but then converged to the latter, implying different cellular processes occurred at the early stages of adaptation.

#### ACKNOWLEDGEMENTS

The authors thank Dr. Dirk Heering (Delft University of Technology, Delft, the Netherlands) for providing UTILS software. This work was supported by HKUST Allocation for School Based Initiative SBI 07/08.SC07.

#### References

1. K. Bagramyan, A. Galstyan and A. Trchounian, *Bioelectrochemistry*, 51 (2000) 151.
2. V. A. Bespalov, I. B. Zhulin and B. L. Taylor, *Proc. Natl. Acad. Sci. U.S.A.*, 93 (1996) 10084.
3. S. J. Ahn and R. A. Burne, *J. Bacteriol.*, 189 (2007) 6293.
4. J. Green and M. S. Paget, *Nat. Rev. Microbiol.*, 2 (2004) 954.
5. Z. Lewandowski, W. Dickinson and W. Lee, *Wat. Sci. Tech.*, 36 (1997) 295.
6. M. R. de Graef, S. Alexeeva, J. L. Snoep and M. J. T. de Mattos, *J. Bacteriol.*, 181 (1999) 2351.
7. P. Whelan, L. E. P. Dietrich and D. K. Newman, *J. Bacteriol.*, 189 (2007) 6372.
8. O. N. Oktyabrsky and G. V. Smirnova, *Acta Biotechnol.*, 9 (1989) 203.
9. J. D. ShROUT and G. F. Parkin, *Water Res.*, 40 (2006) 1191.
10. S. Fetzner and R. Conrad, *Arch. Microbiol.*, 160 (2004) 108.
11. R. P. Buck and P. Vanýsek, *J. Electroanal. Chem.*, 292 (1990) 73.
12. H. Ohshima and T. Kondo, *Biophys. Chem.*, 38 (1990) 177.
13. T. A. Fowler, P. R. Holmes and F. K. Crundwell, *Appl. Environ. Microbiol.*, 65 (1999) 2987.
14. S. Baatout, P. De Boever and M. Mergeay, *Appl. Biochem. Micro+*, 42 (2006) 369.
15. T. A. Gianoulis, J. Raes, P. V. Patel, R. Bjornson, J. O. Korbel, I. Letunic, T. Yamada, A. Paccanaro, L. J. Jensen, M. Snyder, P. Bork and M. B. Gerstein, *Proc. Natl. Acad. Sci. U.S.A.*, 106 (2009) 1374.
16. J. F. Allen, *J. Theor. Biol.*, 165 (1993) 609.
17. L. Ghindilis, P. Atanasov and E. Wilkins, *Electroanal.*, 9 (2005) 661.
18. X. H. Xie, E. L. Li and Z. K. Tang, *Electrochem. Commun.* 12 (2010) 600.
19. X. H. Xie, E. L. Li and Z. K. Tang, *Int. J. Electrochem. Sci.*, 5 (2010) (Accepted)
20. S. Spiro and J. R. Guest, *Trends Biochem. Sci.*, 16 (1991) 310.
21. T. Zhang, C. Z. Cui, S. L. Chen, X. P. Ai, H. X. Yang, P. Shen and Z. R. Peng, *Chem. Commun.*, 21 (2006) 2257.
22. Y. Qiao, C.M. Li, S. J. Bao, Z. S. Lu and Y. H. Hong, *Chem. Commun.*, 11 (2008) 1290.
23. Y. F. Wang, S. Tsujimura, S. S. Cheng and K. Kano, *Appl. Microbiol. Biot.*, 76 (2007) 1439.
24. Camilli and B. L. Bassler, *Science*, 311 (2006) 1113.
25. M. E. Hernandez and D. K. Newman, *Cell. Mol. Life. Sci.*, 58 (2001) 1562.
26. K. Y. Alam and D. P. Clark, *J. Bacteriol.*, 171 (1989) 6213.

27. H. M. Jonkers, M. J. E. C. van der Maarel, H. van Gemerden and T. A. Hansen, *FEMS Microbiol. Lett.*, 36 (1996) 283.
28. B. A. Averill, *Chem. Rev.*, 96 (1996) 2951.
29. G. Unden and J. Bongaerts, *Biochim. Biophys. Acta*, 1320 (1997) 217.
30. C. Condon, R. Cammack, D. S. Patil and P. Owen, *J. Biol. Chem.*, 260 (1985) 9427.
31. S. Iuchi and E. C. C. Lin, *Mol. Microbiol.*, 9 (1993) 9.
32. K. Rabaey, N. Boon, M. Hofte and W. Verstraete, *Environ. Sci. Technol.*, 39 (2005) 3401.
33. E. Marsili, D. B. Baron, I. D. Shikhare, D. Coursolle, J. A. Gralnick and D. R. Bond, *Proc. Natl. Acad. Sci. U.S.A.*, 105 (2008) 3968.
34. D. K. Newman and R. Kolter, *Nature*, 405 (2000) 94.
35. C. E. Turick, F. Caccavo and L. S. Tisa, *FEMS Microbiol. Lett.*, 220 (2003) 99.
36. C. E. Turick, L. S. Tisa and F. Caccavo, *Appl. Environ. Microbiol.*, 68 (2002) 2436.
37. M. F. J. M. Verhagen, E. T. M. Meussen and W. R. Hagen, *Biochim. Biophys. Acta*, 1244 (1995) 99.
38. C. Vedhi, R. Eswar, H. G. Prabu and P. Manisankar, *Int. J. Electrochem. Sci.*, 3 (2008) 509.
39. M. Pandurangachar, B. E. K. Swamy, B. N. Chandrashekar and B.S. Sherigara, *Int. J. Electrochem. Sci.*, 4 (2009) 1319.
40. S. Chitravathi, B. E. K. Swamy, E. Niranjana, U. Chandra, G. P. Mamatha and B.S.Sherigara, *Int. J. Electrochem. Sci.*, 4 (2009) 223.
41. N. Chowdappa, B. E. K. Swamy, E. Niranjana and B.S. Sherigara, *Int. J. Electrochem. Sci.*, 4 (2009) 425-434.
42. K. R. Mahanthesha, B. E. K. Swamy, U. Chandra, Y. D. Bodke, K. V. K. Pai and B. S. Sherigara, *Int. J. Electrochem. Sci.*, 4 (2009) 1237.
43. J. G. Manjunatha, B. E. K. Swamy, G. P. Mamatha, U. Chandra, E. Niranjana, and B. S. Sherigara, *Int. J. Electrochem. Sci.*, 4 (2009) 187.
44. J. G. Manjunatha, B. E. K. Swamy, G. P. Mamatha, S. S. Shankar, O. Gilbert, B. N. Chandrashekar and B. S. Sherigara, *Int. J. Electrochem. Sci.*, 4 (2009) 1469.
45. U. Chandra, B. E. K. Swamy, O. Gilbert, S. S. Shankar, K. R. Mahanthesha and B. S. Sherigara, *Int. J. Electrochem. Sci.*, 5 (2010) 1.
46. J. G. Manjunatha, B. E. K. Swamy, G. P. Mamatha, O. Gilbert, M. T. Shreenivas and B. S. Sherigara, *Int. J. Electrochem. Sci.*, 4 (2009) 1706.
47. N. Jia, Z. Wang, G. Yang, H. Shen and L. Zhu, *Electrochem. Comm.*, 9 (2007) 233.
48. J. M. Myers and C. R. Myers, *J. Bacteriol.*, 182 (2000) 67.
49. V. Stewart, Y. Lu and A. J. Darwin, *J. Bacteriol.*, 184 (2002) 1314.
50. D. P. Lies, M. E. Hernandez, A. Kappler, R. E. Mielke, J. A. Gralnick and D. K. Newman, *Appl. Environ. Microbiol.*, 71 (2005) 4414.
51. C. Roseand and F. B. Edmond, *Langmuir*, 13 (1997) 559.
52. T. M. Nahira and E. F. Bowden, *J. Electroanal. Chem.*, 410 (1996) 9.
53. C. Léger, A. K. Jones, S. P. J. Albracht and F. A. Armstrong, *J. Phys. Chem. B*, 106 (2002) 13058.
54. W. J. Albery, P. N. Bartlett, C. P. Wilde and J. R. Darwent, *J. Am. Chem. Soc.*, 107 (1985) 1854.
55. D. Pan, D. Hu and H. P. Lu, *J. Phys. Chem. B*, 109 (2005) 16390.
56. C. Yeh and G. Hummer, *Proc. Natl. Acad. Sci. U.S.A.*, 101 (2004) 12177.
57. T. Yeung, G. E. Gilbert, J. Shi, J. Silvius, A. Kapus and S. Grinstein, *Science*, 319 (2008) 210.